

# A non-destructive method for mapping formation damage

M.A. Khan <sup>a,\*</sup>, S.Z. Jilani <sup>b,c</sup>, H. Menouar <sup>c</sup>, A.A. Al-Majed <sup>b,c</sup>

<sup>a</sup> Center for Applied Physical Sciences, The Research Institute, King Fahd University of Petroleum and Minerals, KFUPM Box 1947, Dhahran 31261, Saudi Arabia

<sup>b</sup> Department of Petroleum Engineering, King Fahd University of Petroleum and Minerals, Dhahran 31261, Saudi Arabia

<sup>c</sup> Center for Petroleum and Minerals, The Research Institute, King Fahd University of Petroleum and Minerals, Dhahran 31261, Saudi Arabia

Received 19 February 2001; accepted 28 March 2001

## Abstract

Applicability of an ultrasonic method for non-destructive mapping of formation damage is reported for the first time. Oil-saturated and ‘mud’-damaged Berea rock samples were prepared in the laboratory using a leak-off apparatus and machined dry rocks. The depth of ‘mud invasion’ was monitored under varying conditions of overbalanced pressure  $\Delta P$  and contamination time  $\Delta T$ . An interesting observation is that a region of  $\Delta P \sim 2.07 \times 10^3$  kPa produces minimum invasion depth under the conditions investigated. The results are discussed in the context of horizontal wells. © 2001 Elsevier Science B.V. All rights reserved.

PACS: 81.70 Dw; 43.35+d; 91.60 Lj; 62.65+k

Keywords: Formation damage; Mud-invasion depth; Ultrasonic mapping; Non-destructive evaluation; Horizontal wells

## 1. Introduction

Vertical wells have been commonly used to extract oil from geological structures since the early days of commercial exploitation of oil. On the other hand, the idea of horizontal wells initiated some 20 years ago offers many advantages. For instance, horizontal wells produce three to five times more oil than vertical wells on the average. Furthermore, the use of horizontal wells alleviates unwanted production of water and gas, and provides better sweep efficiency and sand problem attenuation. However, one of the main disadvantages of horizontal wells is that they are prone to more formation damage than vertical wells.

Oil is extracted from a reservoir by creating a pressure gradient. According to Darcy’s law [1], oil moves from regions of the reservoir where the pressure is high to the wells where the pressure is low. The oil production rate is in fact inversely proportional to the oil viscosity. Furthermore, it is directly proportional to the magnitude of the pressure gradient, and to the permeability of the formation. However, permeability is a characteristic

of the formation, and can be altered locally during drilling operations. A decrease of the permeability, also called formation damage, results in a decrease of the oil well productivity. It may be noted that formation damage depends not only on the permeability decrease but also on the geometric extent of the damaged area.

A key parameter in quantifying formation damage is the skin parameter  $S$ , defined as [2]

$$S = (\kappa/\kappa_d - 1) \ln(r_d/r_w), \quad (1)$$

where  $\kappa$  is the reservoir permeability,  $\kappa_d$  the damaged-zone permeability,  $r_w$  the well radius, and  $r_d$  the damaged-zone radius. This parameter is used directly in the transient flow equations [3] to estimate the oil production rate in wells that have been affected by formation damage. In general, for a damaged well, the higher the skin  $S$ , the more constricted is the oil production rate.

Different drilling fluids are used to facilitate the drilling process. Invasion of fine particles from the drilling fluids into the formation, also called the ‘mud invasion’, blocks the pores or at least narrows them down. This causes a decrease in the permeability of the formation thereby resulting in a decrease of the production rate when the well is put ‘on stream’. The economic consequences of formation damage justify a thorough study of this problem in order to find ways and means to minimize its effects.

\* Corresponding author. Tel.: +966-3-860-4364/5644; fax: +966-3-860-4281.

E-mail address: aslamk@kfupm.edu.sa (M.A. Khan).

Indeed, numerous studies have been carried out to date to address different aspects of this problem [4–9]. Reference may be made to some review articles [5–7] and books [2,3] for details.

To the best of our knowledge, the present paper is the first report on the applicability of a non-destructive method based on ultrasonic transmission to investigate the invasion depth of drilling-fluid particles as well as other fluids in the drilling process, work-over and completion operations. We have applied this method to map the formation damage in specially prepared Berea rock samples. The results could be used to estimate the skin parameter  $S$  that is crucial for the evaluation of the productivity of the well after it has been completed or repaired during the work-over operations.

## 2. Sample preparation

A leak-off experimental set-up was designed to simulate the drilling-fluid circulation process at the formation face in the well bore under bottom hole conditions. This consisted of a Hassler type core holder that could accommodate cylindrical rock samples up to 30 cm long

and 5.08 cm diameter [10]. The core (rock sample) was mounted inside the rubber sleeve and subjected to an overburden (confining) pressure. One end piece of the core holder had two ports (inlet and outlet), and is referred to as the injection end. The two ports were used to circulate the drilling fluids across the face of the core, and to inject oil and brine as well. The other end piece, known as the production end, had only one port to collect the filtrate, and/or oil, and/or brine, pumped from the injection end. A 10-mm thick ring-shaped stainless steel spacer was placed between the core face and the injection end to allow the mud to circulate and form 'cake' on the core face (Fig. 1a).

Back-pressure regulators (BPR) were installed at each end to control and maintain the desired overbalanced and pore pressure in the system. A differential pressure transducer was also mounted on the core holder for measurement of differential pressures across the core. A fraction collector was used to collect the production fluids in 10 cm<sup>3</sup> test tubes.

Water based polymeric drilling fluid and 33.5° API Arabian medium crude oil with 3.5% KCl brine were used in the experiments reported here. The exact composition and other properties of the water based poly-

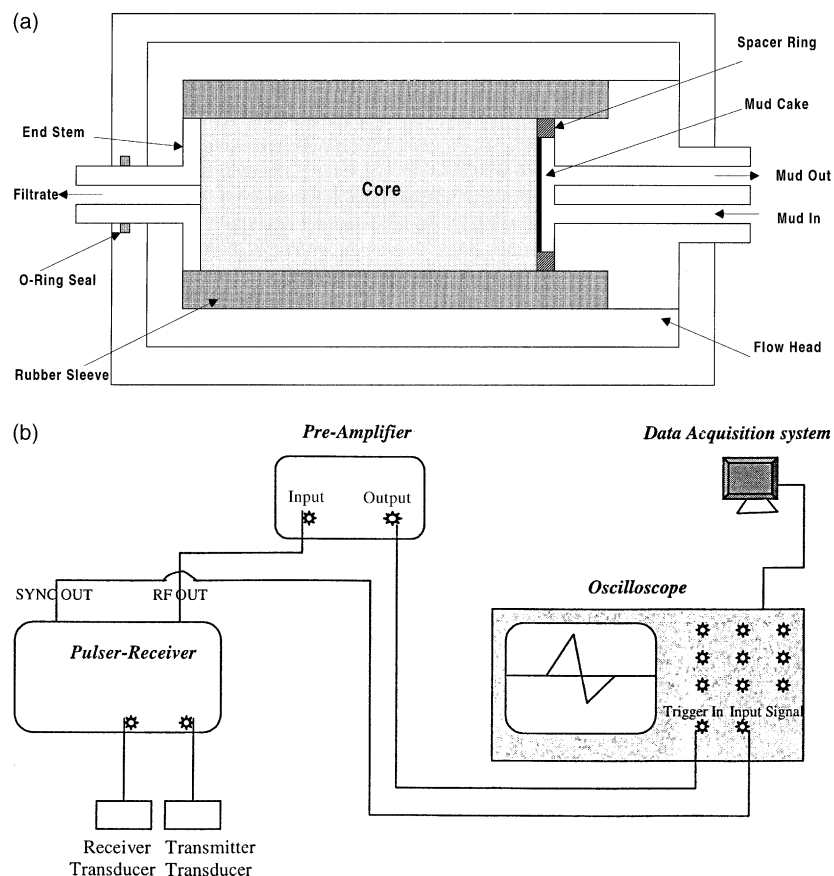


Fig. 1. (a) Hassler type core holder. (b) Schematic diagram showing the experimental arrangement for monitoring ultrasonic wave propagation in prepared Berea samples.

Table 1  
Drilling fluid composition

Water, cm <sup>3</sup>	1096
KCl, g	133
XC-Polymer, g	5.0
Disprac, g	1.7
Dextrid, g	20
KOH, g	1.0
CaCO <sub>3</sub> (fine), g	16.7

Table 2  
Drilling fluid properties

Density, g/cm <sup>3</sup>	1.09
Fluid loss, (ml per 30 min) through no. 50 filter paper	6.7
pH	9.77
Apparent viscosity, cP	31.5
Plastic viscosity, cP	19.0
Yield point, cP	25

meric drilling fluid used are summarized in Tables 1 and 2 respectively.

Berea sandstone cores were machined to the desired size. Their dry weights, dimensions, gas porosities, and gas permeabilities were determined. These cores were evacuated for 8 h in a saturator before being soaked with the prepared brine for 12 h under  $1.72 \times 10^4$  kPa pressure as per API recommended procedure.

Pore- and particle-size distributions in the dry samples were determined as a preliminary test measurement using centrifugal method and image analyzer respectively. The brine saturated Berea core was mounted inside the core holder and flooded with brine at a constant flow rate until steady state was achieved to absolute permeability under reservoir conditions. After flooding with brine, filtered crude oil was passed through the core at a very slow rate to displace the brine in order to get irreducible water saturation  $S_{wj}$ . Initial oil permeability of the core was also measured by flowing crude oil through the core and measuring the flow rates and differential pressures under steady state conditions.

Subsequently, the drilling fluid was circulated across the oil- and water-saturated core at a constant flow rate of 1.0 cm<sup>3</sup>/min. With the start of the circulation, particles in the drilling fluid begin to form a ‘mud cake’ on the face of the core, and the fine particles as well as the filtrate also starts penetrating the core. This pushed the oil and the effluent was collected from the production end in the fraction collector. The core may now be considered damaged with invading filtrate and mud particles.

Drilling fluid was circulated for different periods of time  $\Delta T$  with different overbalanced pressures  $\Delta P$ . A total of 11 different samples of varying lengths were investigated. The lengths of the cores were selected from 10.2 to 25.4 cm to investigate the effects of  $\Delta T$ , and  $\Delta P$ .

Return oil permeability of the damaged core was determined by flowing oil in the opposite direction at a constant flow rate.

### 3. Experimental details for ultrasonic mapping

The experimental set-up for ultrasonic mapping of the formation damage consisted of two panametric transducers (model V403) used to launch and receive longitudinal ultrasonic waves using a panametric pulser-receiver (model 5072). The transmitted signals were amplified by a panametric pre-amplifier and recorded on a 500 MHz digital oscilloscope (HP 54615B) and a personal computer (Fig. 1b). Refined petroleum jelly was used as couplant.

In principle, it is possible to carry out in situ measurements of mud invasion using the ultrasonic technique discussed in this paper. However, complications could arise due to the changes in the velocity of ultrasound resulting from the changes in the density through mud invasion as well as the stress-induced changes in the density. The latter may be caused by the over balance pressure  $\Delta P$  existing between the two faces of the specimen in the experimental set-up that primarily forces the mud as well as the filtrate through the specimen. This stress-induced change in the velocity of the ultrasonic wave is expected to vary along the length of the sample as we move from the high-pressure end to the low-pressure end [11–14]. In order to eliminate this stress-induced velocity variation, we carried out ex situ measurements on each sample mounting it on a separate platform for mapping the mud-invasion profiles while it was held upright without any pressure or stress. Indeed, these measurements were made after preparing the samples under different conditions of overbalance pressure  $\Delta P$  and contamination time  $\Delta T$ , as discussed below. The transmitting and receiving transducers were always kept coaxial with the help of a contoured aligning support-plate fixed to an optical table with adjustable height while moving this support plate up and down in a controlled manner through small steps.

Cylinder-shaped rock samples 5.08 cm in diameter but having different lengths were investigated by sending ultrasonic waves along the diameter at different positions spanning the entire length with a 0.5 cm resolution. Up to 64 signals were averaged to minimize the noise level. The transit times of the waves travelling from the source to the receiver at different positions along the length were stored in the computer. Velocities of the longitudinal ultrasonic waves were determined simply by calculating the ratios of the specimen thickness (i.e., the diameter) and the transit times.

For each sample, the wave velocities were determined under three different conditions as explained below. However, each sample was always kept in a particular

orientation with the help of a reference line marked on the sample and the platform. This was to ensure that the pore orientations do not change for one particular specimen during the course of measurements under dry, oil-saturated and mud-damaged conditions. Furthermore, the thick end was always kept up with the lean end being down. However, some preliminary checks with reversed orientation with respect to the lean and thick ends confirmed that this did not cause any measurable change in the overall mud-invasion profile.

### 3.1. Dry samples

Initially, the core samples were completely dry and the pores inside the sample were presumably filled with air. This gave the reference velocities of the ultrasonic waves for the particular sample under dry conditions at different locations along the length. Any significant change in the measured velocity should indicate the presence of considerable levels of inhomogeneities or voids. However, no real inhomogeneities were detected in the samples under study here.

The mean velocity of ultrasonic waves in dry samples is expected to be lower than the corresponding velocities in oil-saturated and mud-damaged samples. Since ultrasound attenuates exponentially in air, it is understood that the waves essentially follow a zig-zag path going around the pores in the rock matrix instead of a direct path to reach the other end. Thus, the actual path length increases and the waves take more time to reach the receiver. This shows through a decrease in the velocity.

### 3.2. Oil-saturated samples

In the second step, the dry samples were completely saturated with brine that was subsequently displaced by crude oil to get irreducible water  $S_{wi}$  and initial oil  $S_{oi}$  in place. The mean velocity in this case should be higher than the case of dry samples because now the waves can follow a straight path through the sample since the pores are essentially filled with a liquid. Velocities at this stage are considered as base-line velocity.

### 3.3. Mud-damaged samples

In the third step, the oil-saturated core samples discussed in Section 3.2 above were exposed to the circulating drilling fluid at the face of the core under different conditions of overbalance pressure  $\Delta P$  and contamination time  $\Delta T$ . In the process, the particulates (i.e., fine particles constituting the mud) and the filtrate in the drilling fluid penetrate the sample core, as noted earlier. These invading particles are expected to clog the pores and/or pore throats, after sticking there. Since solids generally exhibit higher wave velocities than liquids, so ultrasonic waves will travel faster through the pores

plugged by the solid particulate. Thus, one can get higher mean velocity for mud-damaged sample than the previous two cases. However, the ‘primary’ pores in the original dry rock are understood to be filled by the mud that itself may have some ‘secondary’ pores albeit much smaller in size than the ‘primary’ pores. Furthermore, these ‘secondary’ pores may also be filled with a fluid (filtrate or the original oil etc.). In this sense the composite picture is quite complicated.

At this stage, the core is damaged and its permeability is reduced. The corresponding wave velocities were again measured through the damaged cores, as mentioned earlier.

## 4. Results and discussion

The structure of rocks is expected to be quite complex. There may be some inhomogeneities in the material composition, grain sizes and their shapes, pore sizes and their orientations, and their distributions within the rock samples. Furthermore, there is the possibility of partial saturation of the pores with the mud and fluids (oil, water, or filtrate in liquid and gaseous phase). However, as mentioned earlier, no significant inhomogeneities were found in the samples under study.

Mathematically, the velocity in the oil-saturated or ‘mud’-damaged samples at a particular point can be calculated from

$$t = L/v = \sum L_i/v_i \quad (2)$$

where  $t$  is the total transit time of the wave,  $L$  the total length of the sample,  $L_i$  the part length occupied by the material  $i$  (rock grain, mud, oil, etc),  $v$  the average ultrasonic velocity through the sample, and  $v_i$  the ultrasonic velocity through the part length occupied by the material  $i$ .

For each sample core, the velocities were measured under the three different conditions discussed in Section 3 above, and at up to 47 different positions along the length of the core, depending on the total length. These were plotted in simple graphs to obtain unambiguous information about the mud-invaded portion of the sample.

The depths of mud invasion in the sample cores for different overbalanced pressures and contamination times were measured through ultrasonic velocity profiles along the length of the core. Fig. 2a presents a typical velocity profile for the core prepared with  $\Delta P = 2.07 \times 10^3$  kPa and  $\Delta T = 12$  h. The velocity distributions at the three stages; dry, oil and water saturated (at  $S_{oi}$  and  $S_{wi}$ ), and mud-laden sample are quite distinct. The average velocity in the dry rock is 1990 m/s while for oil-saturated sample the average velocity is about 30% higher, i.e., 2580 m/s. In this figure, the velocity in

the dry rock sample has been multiplied by a factor of 1.25 to highlight the comparison between the mud-invaded sample and the oil-saturated sample. The velocity profile for oil-saturated sample acts as the base-line velocity distribution. As expected, the mud-laden portion of the sample core shows higher velocities. We note that initially (seen from the right side, or the dense end) there

is a plateau where the average velocity is about 3% higher than the base-line velocity. This region is followed by a linear decrease in the velocity. The plateau indicates that this part is essentially completely filled with the mud particles and the filtrate, while the linear decrease in velocity is due to a gradual decrease in these particles and filtrate concentration (i.e. incomplete invasion).

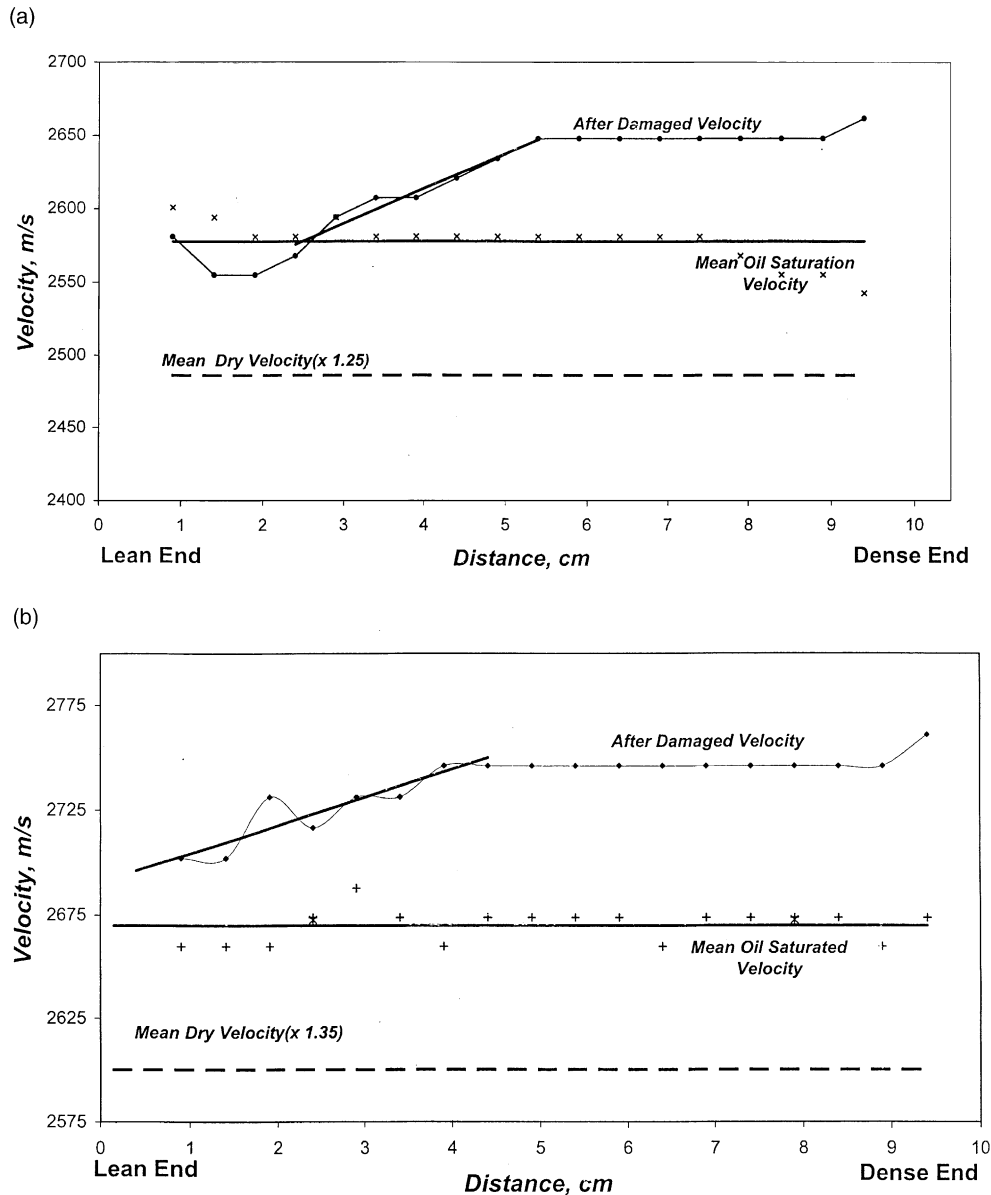


Fig. 2. (a) A typical velocity profile for the 10-cm long Berea core prepared with overbalanced pressure  $\Delta P = 2.07 \times 10^3$  kPa and contamination time  $\Delta T = 12$  h. The velocity in the dry rock has been multiplied by a factor of 1.25 to highlight the comparison between the mud-invaded and the oil-saturated sample. (b) Velocity profile for the 10-cm long Berea core prepared with overbalanced pressure  $\Delta P = 4.83 \times 10^3$  kPa and contamination time  $\Delta T = 24$  h. The velocity in the dry rock has been multiplied by a factor of 1.35 to highlight the comparison between the mud-invaded and the oil-saturated sample. (c) Velocity profile for the 10-cm long Berea core prepared with overbalanced pressure  $\Delta P = 2.07 \times 10^3$  kPa and contamination time  $\Delta T = 4$  h. The velocity in the dry rock has been multiplied by a factor of 1.25 to highlight the comparison between the mud-invaded and the oil-saturated sample. (d) Velocity profile for the 10-cm long Berea core prepared with overbalanced pressure  $\Delta P = 0.69 \times 10^3$  kPa and contamination time  $\Delta T = 24$  h. The velocity in the dry rock has been multiplied by a factor of 1.15 to highlight the comparison between the mud-invaded and the oil-saturated sample.

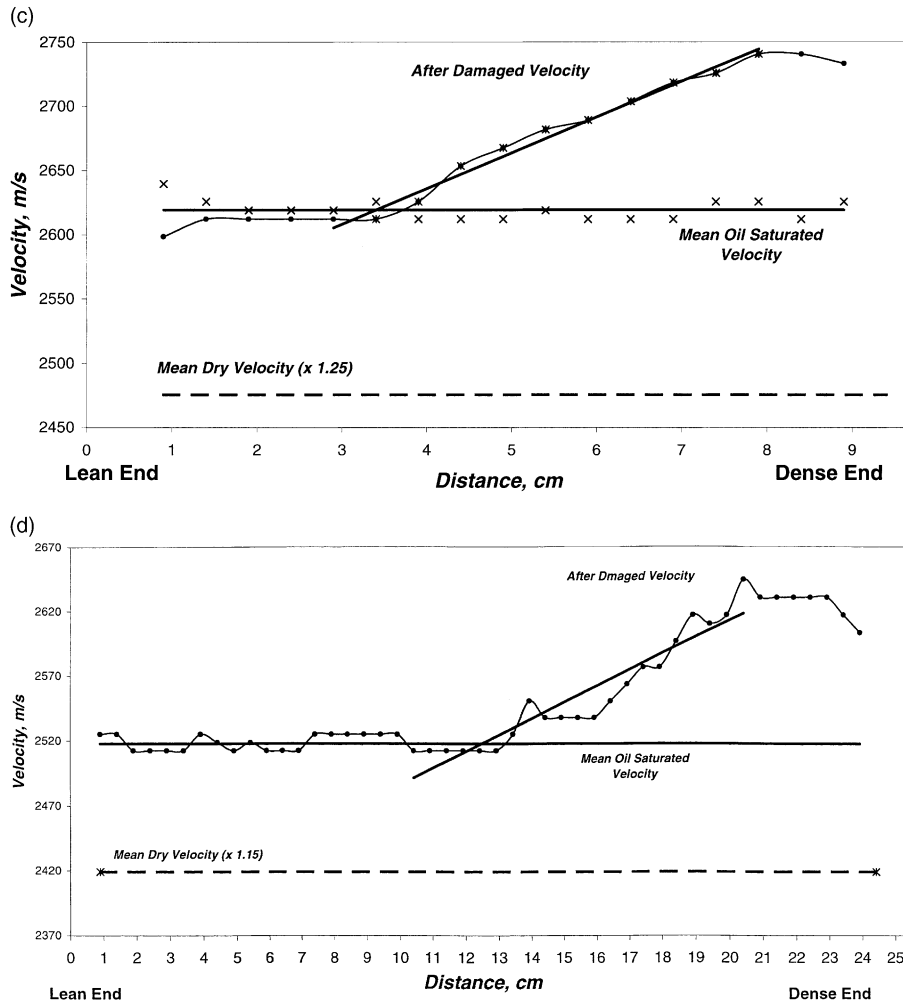


Fig. 2 (continued)

Apparently, the remaining portion of the sample leading to the lean end may not be affected by the mud.

When the velocity in the mud-damaged sample becomes equal to the reference velocity, this may imply that this region remains unaffected in as far as mud or filtrate invasion is concerned. Accordingly, the invasion depth of the mud can be measured easily from the velocity profile, and the region occupied by the filtrate can also be seen.

Fig. 2b shows an example of a nearly full-length invasion of 'mud' under  $\Delta P = 4.83 \times 10^3$  kPa and  $\Delta T = 24$  h. Here the region with pores exclusively filled by the filtrate (without the fine particles constituting the mud) is not visible.

It is further noted that towards the lean end of the sample, the velocity profile shows some mixed behavior. Normally, one would expect that the velocity in the mud-damaged samples should be either higher or equal to the base-line velocity (oil-saturated case) within the statistical error margin. But in some of the mud-damaged samples (Fig. 2a), it is seen to be actually less than

the base-line velocity, while in some other cases it could be slightly higher than the base-line velocity. In most cases, however, the velocity change was seen to be within the noise level (see Fig. 2c, representing the data for  $\Delta P = 2.07 \times 10^3$  kPa and  $\Delta T = 4$  h; and Fig. 2d, representing the data for  $\Delta P = 0.69 \times 10^3$  kPa and  $\Delta T = 24$  h).

Interplay between several different processes comes into consideration here. Firstly, since the sample is held vertically with the dense end up during the ultrasonic measurements, gravity might induce some accumulation of fluid/filtrate at the lean end. Furthermore, accumulation of the filtrate fluids through the 'end effect' caused by the viscous forces might also influence the velocity at the lean end. In these two cases, the density of the filtrate compared to the oil and water becomes an important consideration. However, the actual density of the filtrate (after removal of particulates, i.e., mud fines) is slightly higher (specific gravity = 1.083) than the corresponding density of oil/water/brine filling the pores discussed in Section 3.2. This should result in a higher velocity rather

than lower. A further possibility is partial saturation of the pores near the lean end with liquid and gaseous phase (oil, water and/or filtrate) including trapped air. This could be caused by some evaporation of the fluid from this end through extended exposure to ambient atmosphere or in some cases, just an incomplete initial saturation (trapped air etc.), and these would result in a lower velocity. In any case, the time between preparing the mud-damaged sample and subsequently initiating the ultrasonic measurements should be minimum possible to control possible loss of fluid through evaporation.

#### 4.1. Influence of overbalanced pressure ( $\Delta P$ )

We have investigated the influence of increasing overbalanced pressure in the  $6.90 \times 10^2$ – $4.83 \times 10^3$  kPa range while keeping all other parameters constant for different contamination times  $\Delta T$  (Fig. 3). We may look at curve “a” in Fig. 3 which summarizes the influence of increasing  $\Delta P$  on the invasion depths for a fixed contamination time  $\Delta T = 24$  h. One would expect an increase in invasion depth with increasing  $\Delta P$  in the sense that higher pressures would force the mud particles and the filtrate to penetrate deeper into the formation. However, contrary to this expectation, our experiments indicate an initial decrease in the invasion depths when  $\Delta P$  increases from  $6.90 \times 10^2$ – $2.07 \times 10^3$  kPa. But, as  $\Delta P$  increases beyond  $2.07 \times 10^3$  kPa, the invasion depth increases albeit rather slowly, in line with the expectations.

We may note that the invasion depth is considerably higher i.e. 12.9 cm for  $\Delta P = 6.90 \times 10^2$  kPa than for  $\Delta P = 1.38 \times 10^3$  and  $2.07 \times 10^3$  kPa which are 11.3 and 8.31 cm, respectively. Further increases in  $\Delta P$  tend to increase the invasion depth slowly, reaching 11.97 cm for  $4.83 \times 10^3$  kPa. Thus, the region around  $\Delta P =$

$2.07 \times 10^3$  kPa acts as a critical pressure zone which produces minimum invasion depth.

A possible reason for this interesting behavior can be understood from some intuitive arguments as well as some previous observations made by different researchers, even though those observations were made in different contexts. For instance, this can be viewed in terms of some bridging action and entrainment of particles occurring at the pores. The bridging and entrainment actions have been discussed in some detail by Monaghan et al. [15], Krueger et al. [16], Gruebeck and Collins [17], Krueger [5], and Saleh et al. [18]. More specifically, at high-pressure gradients and correspondingly high flow rates, randomly dispersed particles apparently tend to interfere with each other as they approach the pore constrictions and finally cause some sort of bridging action [5,15–18]. On the other hand, at low-pressure gradients, the particles are in more gentle movement and align themselves so that one by one they can work their way through the constrictions without bridging and thus can effect deeper invasion [15–18].

It is believed that at low  $\Delta P$  (e.g.,  $6.90 \times 10^2$  kPa), the mud particles gather themselves loosely at the pore constrictions. These loosely blocking particles allow filtrate and micro-fine particles to pass through them resulting in deeper migration. As  $\Delta P$  increases, these particles start to form relatively tight bridges at the pore throats and begin to act as “one-way check-valves”, thereby allowing less filtrate and micro-fines through them to move into the formation. This is seen through a decrease of the invasion depth when  $\Delta P$  is increased to  $2.07 \times 10^3$  kPa. At  $\Delta P \sim 2.07 \times 10^3$  kPa, particles appear to form a perfect check valve as they develop the tightest bridge at the pore constrictions.

The increase in invasion depth with  $\Delta P$  beyond  $2.07 \times 10^3$  kPa is easier to explain. Overbalanced pressures  $>2.07 \times 10^3$  kPa result in breaking of the tight

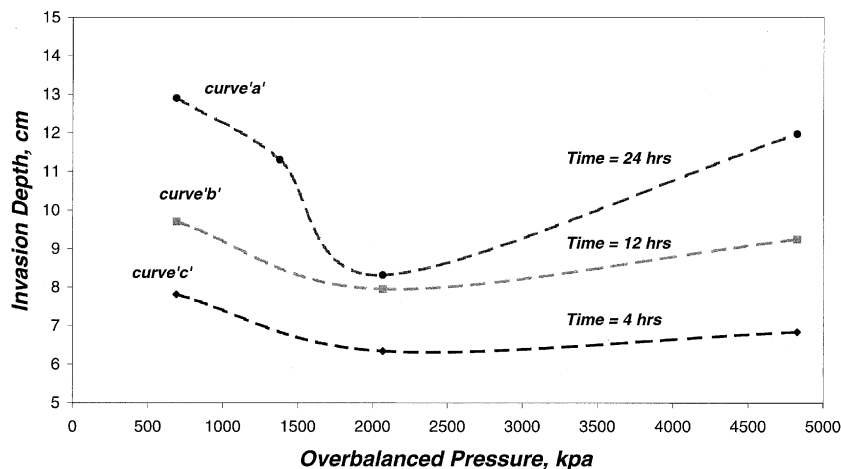


Fig. 3. Effect of overbalanced pressure  $\Delta P$  on the depth of mud invasion for different contamination time  $\Delta T$ .

particle bridges mentioned above. Either these particles break into small sizes or pore constrictions/throats get enlarged by the pressure gradient or by entrainment of some grains from the pore throat walls [17]. This helps the filtrate and the solid particles to migrate deeper into the sample.

The overall behavior generally follows the same general trend in curves “b” and “c” in Fig. 3 corresponding to  $\Delta T = 12$  h and 4 h, respectively.

## 5. Conclusion

We have, for the first time, demonstrated the applicability of ultrasonic mapping of formation damage. A parametric study was carried out on the depth of mud invasion under different conditions of overbalanced pressure and contamination times. A minimum invasion depth is observed around a critical overbalanced pressure  $\sim 2.07 \times 10^3$  kPa. This has been explained in terms of bridging and entrainment action of the particles under certain conditions of overbalance pressure. The results may have some important applications for some oil-field operations particularly in the context of horizontal wells.

## Acknowledgements

The support provided by the Research Institute of KFUPM is gratefully acknowledged.

## References

- [1] M.F. Hawkins, A note on the skin effect, *Petroleum Transactions of American Institute of Mining, Metallurgical and Petroleum Engineers*, AIME 207 (1956) 356.
- [2] B.C. Craft, M.F. Hawkins, *Applied Petroleum Reservoir Engineering*, second ed., Prentice Hall Inc., 1991, p. 210 (revised by Ronald E. Terry).
- [3] J. Lee, *Well Testing*, SPE Text Book Series, 1982, p. 50.
- [4] E.E. Glenn, M.L. Slusser, Factors affecting well productivity II: drilling particle invasion into porous media, *Petroleum Transactions of American Institute of Mining, Metallurgical and Petroleum Engineers*, AIME 210 (1957) 132.
- [5] R.F. Kruger, An overview of formation damage and well productivity in oilfield operations, SPE-10029, *Journal of Petroleum Technology* 38 (1986) 131.
- [6] K.E. Porter, An overview of formation damage, SPE-19894, *Journal of Petroleum Technology* 41 (1989) 780.
- [7] T. Beatty, B. Hebner, D.B. Benion, Minimizing formation damage in horizontal wells: laboratory and field case studies, *Journal of Canadian Petroleum Technology* 34 (1995) 57.
- [8] J. Yan, G. Jiang, X. Wu, Evaluation of formation damage caused by drilling and completion fluids in horizontal wells, *Journal of Canadian Petroleum Technology* 36 (1997) 36.
- [9] J.D. Lynn, Drilling damage associated with water-based fluids, *Saudi Aramco Journal of Technology* (1998) 30.
- [10] N.G. Gruber, K.L. Adair, New laboratory procedures for evaluation of drilling induced formation damage and horizontal well performance, *Journal of Canadian Petroleum Technology* 34 (1995) 27.
- [11] C.M. Sayers, J.G. Van Munster, M.S. King, Stress-induced ultrasonic anisotropy in Berea sandstone, *International Journal of Rock Mechanics and Mining Sciences & Geomechanics Abstracts* 27 (1990) 429.
- [12] S.L. Ita, N.G.W. Cook, L.R. Myer, K.T. Nihei, Effects of stress anisotropy on the static and dynamic properties of Berea sandstone, *International Journal of Rock Mechanics and Mining Sciences & Geomechanics Abstracts* 30 (1993) 785.
- [13] G. Tao, M.S. King, M. Nabibidhendi, Ultrasonic wave-propagation in dry and brine-saturated sandstones as a function of effective stress: laboratory measurements and modeling, *Geophysical Prospecting* 43 (1995) 299.
- [14] A.K. Benson, J. Wu, A modeling solution for predicting (a) dry rock bulk modulus, rigidity modulus and (b) seismic velocities and reflection coefficients in porous fluid-filled rocks with applications to laboratory rock samples and well logs, *Journal of Applied Geophysics* 41 (1999) 49.
- [15] P.H. Monaghan, R.A. Salathiel, B.E. Morgan, A.D. Kaiser, Laboratory studies of formation damage in sands containing clay, *Petroleum Transactions of American Institute of Mining, Metallurgical and Petroleum Engineers*, AIME 216 (1959) 209.
- [16] R.F. Krueger, L.C. Vogel, P.W. Fisher, Effect of pressure drawdown on clean-up of clay- or silt- blocked sandstone, *Journal of Petroleum Technology* 19 (1967) 379.
- [17] C. Gruebeck, R.E. Collins, Entrainment and deposition of fine particles in porous media, *Society of Petroleum Engineers Journal* 22 (1982) 847.
- [18] S.T. Saleh, R. Rustam, W. El-Rabaa, M.R. Islam, Formation damage study with a horizontal wellbore model, *Journal of Petroleum Science and Engineering* 17 (1997) 87.